and red-shifted emission may then also occur through a L_a-type state which is stabilized by a large backbone dipole moment and is strongly coupled to the initially excited L_b levels through the peptide backbone coordinates.

Summary

Fluorescence spectroscopy has revealed that two distinct types of conformers are present in the isolated dipeptides Trp-Gly and Gly-Trp in a supersonic expansion. One type of conformer exhibits sharp resonance fluorescence from the excited indole chromophore of the tryptophyl residue, while the other type of conformer shows only broad fluorescence with a maximum shifted approximately 3000 cm^{-1} from the excitation frequency. In analogy with work on several tryptophan derivatives, the existence of a broad emitting conformer appears to require the formation of an intramolecular hydrogen bond in the peptide backbone. In these dipeptides, the terminal amine may hydrogen bond to either the carboxylic acid or the amide proton and work on derivatives of the two peptides has been used to isolate the contribution from the amide hydrogen-bonded species. Here it is found that only the Trp-Gly derivative exhibits the exciplex-like fluorescence. These results appear to be consistent with a dipole-induced perturbation to the indole chromophore which originates from a high dipole, hydrogen-bonded conformation of the peptide backbone.

Acknowledgment. This work was supported by the National Science Foundation under Grants CHE-8311971 and CHE-8818321 and by the NSF-MRL.

Registry No. Gly-Trp, 2390-74-1; Trp-Gly, 7360-09-0; Trp-Gly-Gly, 20762-31-6; Trp-NHMe, 53708-63-7; glycyltryptamine, 122902-82-3.

Dissymmetry Effects in μ-Oxo Diiron(III) Species: Structures and Spectroscopic Properties of $[N5FeOFeX_3]^+$ (X = Cl, Br) and Implications for Oxo-Bridged Dinuclear Iron Proteins

Pedro Gômez-Romero,*,† E. H. Witten,‡ William Michael Reiff,‡ Gabriele Backes,§ Joann Sanders-Loehr,§ and Geoffrey B. Jameson*,†

Contribution from the Department of Chemistry, Georgetown University, Washington, D.C. 20057, the Department of Chemistry, Northeastern University, Boston, Massachusetts 02115, and the Department of Chemical and Biological Sciences, Oregon Graduate Center, Beaverton, Oregon 97006-1999. *Received August 15, 1988. Revised Manuscript Received July 7, 1989*

Abstract: We report the first nonbiological unsymmetrical μ-oxo diiron(III) complexes: $[(N5)FeOFeX_3]X$, where N5 is *N*-(hdyroxyethyl)-*N*,*N*',*N*'-tris(2-benzimidazolylmethyl)-1,2-diaminoethane and X is Cl (compound I) or Br (compound II). X-ray crystallographic studies reveal structures in which octahedral and tetrahedral iron atoms are bridged by the oxo group with an Fe-O-Fe angle of 149.5 (3)° for I and 150.6 (4)° for II. A small but significant difference in Fe-O separations is observed in which the longer distances are associated with N5Fe-O [1.784 (4) Å in I, 1.797 (9) Å in II] and shorter distances with X_3Fe-O [1.751 (4) Å in I, 1.726 (9) Å in II]. Unusually strong antiferromagnetic coupling is observed for I [$J = -122$ (1) cm^{-1}] and a more typical value for II [$J = -106$ (1) cm^{-1}]. The nonequivalent iron atoms exhibit distinct Mössbauer spectroscopic parameters for I at 293 K ($\delta = 0.23$, $\Delta E_q = 1.15$ mm/s and $\delta = 0.34$, $\Delta E_q = 1.36$ mm/s), whereas II at 77 K gives an even better resolved pair of doublets ($\delta = 0.31$, $\Delta E_q = 1.41$ mm/s for $FeOBr_3$ and $\delta = 0.41$, $\Delta E_q = 1.22$ mm/s for N5FeO). The resonance Raman spectrum of I shows a band at 850 cm^{-1} (806 cm^{-1} for ^{18}O) assigned to the Fe-O-Fe asymmetric stretch, ν_{as}. Contrary to the behavior of symmetrical dinuclear species, the ν_{as} mode in I and II has more than 2 times the Raman intensity of the symmetric Fe-O-Fe stretch. A stable one-electron-reduced derivative of I is produced by cyclic voltammetry of the compound in acetonitrile. Many properties of the asymmetric μ-oxo diiron(III) complexes are similar to those observed for dinuclear iron proteins (hemerythrin, ribonucleotide reductase, purple acid phosphatase, methane monooxygenase); a comparable inequivalence of the two iron atoms is inferred for several of these proteins.

μ-Oxo diiron(III) complexes have long been of considerable interest for their distinctive magnetic and spectroscopic properties[1] and relevance to non-heme diiron proteins.[2] Whereas almost all of the many synthetic systems are symmetrical and remarkably unreactive species, in the biological systems the diiron μ-oxo motif is unsymmetrical, as inferred from ^{57}Fe Mössbauer spectroscopy, and mediates or is in the vicinity of a variety of biochemical activities. These include oxygen transport (hemerythrin[2,3]), hydrolysis (purple acid phosphatase[2,4]), reduction (ribonucleotide reductase[2,5]), and oxidation (methane monooxygenase[2,6]).

Magnetic susceptibility measurements are a primary means for the identification of the μ-oxo diiron(III) motif in metalloproteins.[2] Singly bridged μ-oxo diiron(III) complexes show substantial coupling, for which, with the possible exception of some porphyrin and phthalocyanine complexes, the values of J ($H = -2JS_1S_2$) lie in the remarkably narrow range of -85 to -110 cm^{-1} regardless of the Fe-O-Fe angle and of the nature and number of donor

* Authors to whom correspondence should be addressed.
† This work constitutes part of the Ph.D. Thesis of Pedro Gômez-Romero. Georgetown University, 1987.
‡ Northeastern University.
§ Oregon Graduate Center.

(1) Murray, K. S. *Coord. Chem. Rev.* **1974**, *12*, 1-35.
(2) (a) Sanders-Loehr, J. In *Iron Carriers and Iron Proteins*; Loehr, T. M., Ed.; VCH: New York, in press. (b) Lippard, S. J. *Angew. Chem., Int. Ed. Engl.* **1988**, *27*, 344-361.
(3) (a) Klotz, I. M.; Kurtz, D. M., Jr. *Acc. Chem. Res.* **1984**, *17*, 16-22. (b) Wilkins, P. C.; Wilkins, R. G. *Coord. Chem. Rev.* **1987**, *79*, 195-214.
(4) (a) Antanaitis, B. C.; Aisen, P. *Adv. Inorg. Biohem.* **1983**, *5*, 111-36. (b) Averill, B. A.; Davis, J. C.; Burman, S.; Zirino, T.; Sanders-Loehr, J.; Loehr, T. M.; Sage, J. T.; Debrunner, P. G. *J. Am. Chem. Soc.* **1987**, *109*, 3760-7.
(5) Sjöberg, B.-M.; Grāslund, A. *Adv. Inorg. Biochem.* **1983**, *5*, 87-110.
(6) (a) Woodland, M. P.; Dalton, H. *J. Biol. Chem.* **1984**, *259*, 53-9. (b) Fox, B. G.; Surerus, K. K.; Münck, E.; Lipscomb, J. D. *J. Biol. Chem.* **1988**, *263*, 10553-5.

0002-7863/89/1511-9039$01.50/0

atoms (4–7).[1,7] Multiply bridged species and metHr show greater coupling with J in the range −117 to −134 cm^{-1}.[8-12] With other bridging ligands, such as hydroxide, alkoxide, or phenoxide, only weak antiferromagnetic coupling (J ca. −10 cm^{-1}) is observed.[13]

More recently, resonance Raman spectroscopy has been used to characterize different forms of the active sites of hemerythrin,[14] ribonucleotide reductase,[15] and model compounds.[8a,16,17] The Fe–O–Fe symmetric and asymmetric stretching modes have been identified at about 400–550 and 750–850 cm^{-1}, respectively, with the former band more strongly enhanced. However, for a purple acid phosphatase no such enhancement was observed, despite magnetic susceptibility evidence for a μ-oxo species.[4b]

We have prepared unsymmetrical diiron(III) μ-oxo systems, [N5FeOFeX$_3$]$^+$, where N5 = *N*-(2-hydroxyethyl)-*N*,*N*′,*N*′-tris-(2-benzimidazolylmethyl)-1,2-diaminoethane, and X = Cl or Br,[18]

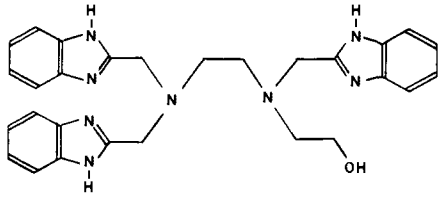

in order to examine the consequences of asymmetry[19] on spectroscopic and magnetic properties. By unsymmetrical we mean that no symmetry or pseudo-symmetry operation, other than the identity operation C_1 (or 1), relates the coordination environment around one iron to that around a second. We find that asymmetry has significant effects on the Mössbauer spectra, vibrational spectra, and antiferromagnetic coupling between the iron atoms; the range of spectroscopic behavior possible for oxo-bridged diiron(III) systems has been extended with important consequences for the proteins.

Experimental Details

Starting Materials. Preparation of Compounds. Starting materials from Aldrich, J. T. Baker, or Fisher were used as purchased without further purification. All solutions of anhydrous $FeBr_3$ (Alfa) were filtered twice to remove particles of metallic iron present as impurities.

Table I. Crystal Data and Data Collection Procedures [N5FeOFeX$_3$]X·2C$_2$H$_5$OH

	X = Cl	X = Br
empirical formula	$Fe_2Cl_4C_{32}H_{42}N_8O_4$	$Fe_2Br_4C_{32}H_{42}N_8O_4$
formula weight	856.24	1034.0
space group	$P2_1/n$	$P2_1/c$
a, Å	15.712 (2)	15.691 (3)
b, Å	13.921 (2)	14.096 (2)
c, Å	19.094 (3)	20.050 (4)
β, deg	111.79 (1)	116.06 (1)
V, Å^3	3878 (2)	3984 (2)
Z	4	4
$d_{calcd(obsd)}$, g/mL	1.467 (1.46)	1.724 (1.69)
cryst shape	wedge-shaped thick plate	oblique thick plate
cryst dimens, mm	ca. 0.4 × 0.2 × 0.1	ca. 0.45 × 0.20 × 0.13
linear abs coeff, cm^{-1}	10.641	47.467
transm factors, %	88.8–99.7 (empir)	75.9–99.8 (empir)
scan type	$\theta/2\theta$	$\theta/2\theta$
scan range	$2.5° < 2\theta < 50.0°$	$2.5° < 2\theta < 45.0°$
sin θ/λ limits, Å^{-1}	0.0307–0.596	0.0307–0.539
data collected	$\pm h,+k,+l$	$\pm h,+k,+l$ and $\pm h,-k,-l$ for $30 < 2\theta < 40$
total no. of reflcns	5558	5288
total no. of unique data	5558	2516
unique data with $F_o^2 > 3\sigma F_o^2$	3834	2019
p ($w = KI/[\sigma^2 \text{count} + (pK)^2]$)	0.040	0.040
data/param	3831/448	2019/425
extincn coeff	not refined	not refined
final R (R_w)	0.055 (0.073)	0.050 (0.058)

Special low-absorption glass and quartz capillaries, used to seal crystals for X-ray crystallography studies, were purchased from the Charles Supper Co.

***N*-(2-Hydroxyethyl)-*N*,*N*′,*N*′-tris(2-benzimidazolylmethyl)-1,2-diaminoethane Tetrahydrochloride (N5·4HCl).** *N*-(hydroxyethyl)-ethylenediaminetriacetic acid (HEDTA; 34.75 g, 0.125 mol) and 54.1 g (0.50 mol) of *o*-phenylenediamine were finely ground, mixed thoroughly, and heated in a paraffin oil bath at 175–190 °C, with stirring. After effervescence ceased (ca. 70 min), the red molten glass was cooled, 130 mL of concentrated HCl was added, and the mixture was stirred at 20 °C for 24 h. The white-blue precipitate was filtered, washed with small amounts of concentrated HCl, slurried with acetone, and then recrystallized twice from 1000 mL of 95% ethanol to give 28.4 g of white powder. Concentration of the mother liquor yielded an additional 5.9 g (total yield up to 41%). Titration with NaOH gave 5.3 (3) mmol of H$^+$/g of sample, consistent with the following formula and analyses. Anal. Calcd for N5·4HCl·2H$_2$O, $C_{28}H_{38}N_8O_3Cl_4$: C, 49.71; H, 5.66; N, 16.56; Cl, 20.96. Found (Mic-Anal): C, 49.70, H, 5.67; N, 16.48; Cl, 20.77. Infrared (KBr, cm^{-1}): 3320 (s), 2850 (vs, br), 1620 (s), 1520 (m), 1490 (m), 1460 (s), 1380 (m), 1225 (s), 1070 (m), 1020 (m), 770 (sh), 755 (s), 620 (m).

***N*-(2-Hydroxyethyl)-*N*,*N*′,*N*′-tris(2-benzimidazolylmethyl)-1,2-diaminoethane (N5).** A 9.764-g sample of the HCl salt was dissolved in 2.5 L of iced water and neutralized with 5.0 mL of concentrated NH$_4$OH, added dropwise with vigorous stirring, yielding a voluminous white precipitate that was filtered and washed repeatedly with large portions of deionized water before drying in air (7.17 g, 100% conversion from the HCl salt, 41% overall yield). Anal. Calcd for N5·2H$_2$O, $C_{28}H_{34}N_8O_3$: C, 63.38; H, 6.46; N, 21.12. Found (Galbraith): C, 63.38; H, 6.29; N, 21.35. Infrared (KBr, cm^{-1}): 3400 (sh), 3100 (vs, br), 2820 (s), 1620 (m), 1530 (m), 1450 (sh), 1430 (s), 1350 (m), 1270 (s), 1110 (m), 1020 (m), 770 (sh), 745 (s). ^{1}H NMR (DMSO-d_6) δ (ppm) (mult, rel. intensity): 7.6 (m, 6), 7.2 (m, 6), 4.16 (s, 6), 4.10 (s, 2), 3.64 (t, 2), 2.99 (s, 2), 2.91 (s, 2), 2.79 (t, 2).

[N5FeOFeCl$_3$]Cl. In a typical preparation, 0.196 g (0.40 mmol) of ligand N5 was added to a solution of 0.217 g (0.80 mmol) of FeCl$_3$·6H$_2$O in 20 mL of 95% ethanol to give a dark red solution that after 1 day produced 0.15 g of large, shiny, dark red crystals (44% yield). The crystals are insoluble in ethanol and slightly soluble in acetonitrile and acetone. In water and DMSO dissociation occurs. Anal. Calcd for [N5FeOFeCl$_3$] Cl·1.5C$_2$H$_5$OH·1.5H$_2$O, $C_{31}H_{42}N_8O_5Cl_4Fe_2$: C, 43.29; H, 4.92; N, 13.02; Cl, 16.49; Fe, 12.99. Found (Galbraith): C, 43.38; H, 4.83; N, 13.00; Cl, 16.58; Fe, 12.29. Found (E+R): Fe, 12.45. Infrared (KBr, cm^{-1}): 3520 (sh), 3330 (s), 3060 (s), 2980 (s), 2920 (s, br), 2770 (sh), 2640 (sh), 1620 (m), 1595 (m), 1545 (m), 1495 (s), 1480

(7) (a) Ou, C. C.; Wollmann, R. G.; Hendrickson, D. N.; Potenza, J. A.; Schugar, H. J. *J. Am. Chem. Soc.* **1978**, *100*, 4717–24. (b) Drew, M. G. B.; McKee, V.; Nelson, S. M. *J. Chem. Soc., Dalton Trans.* **1978**, 80–4. (c) takahashi, K.; Nishida, Y.; Maeda, Y.; Kida, S. *J. Chem. Soc., Dalton Trans.* **1985**, 2375–80.

(8) (a) Armstrong, W. H.; Spool, A.; Papaefthymiou, G. C.; Frankel, R. B.; Lippard, S. J. *J. Am. Chem. Soc.* **1984**, *106*, 3653–67. (b) Armstrong, W. H.; Lippard, S. J. *J. Am. Chem.* Soc. **1984**, *106*, 4632–3.

(9) (a) Wieghardt, K.; Pohl, K.; Gebert, W. *Angew. Chem., Int. Ed. Engl.* **1983**, *22*, 727. (b) Wieghardt, K.; Pohl, K.; Ventur, D. *Angew. Chem., Int. Ed. Engl.* **1985**, *24*, 392–3. (c) Chaudhuri, P.; Wieghardt, K.; Nuber, B.; Weiss, J. *Angew. Chem., Int. Ed. Engl.* **1985**, 778–9.

(10) Toftlund, H.; Murray, K.; Zwack, P. R.; Taylor, L. F.; Anderson, O. P. *J. Chem. Soc., Chem. Commun.* **1986**, 191–3.

(11) Gómez-Romero, P.; Casañ-Pastor, N.; Ben-Hussein, A.; Jameson, G. B. *J. Am. Chem. Soc.* **1988**, *110*, 1988–90.

(12) Dawson, J. W.; Gray, H. B.; Hoenig, E.; Rossman, G. R.; Schredder, J. M.; Wang, R.-H. *Biochemistry* **1972**, *11*, 461–5.

(13) (a) Ou, C. C.; Lalancette, R. A.; Potenza, J. A.; Schugar, H. J. *J. Am. Chem. Soc.* **1978**, *100*, 2053–7, and references cited therein. (b) Armstrong, W. H.; Lippard, S. J. *J. Am. Chem. Soc.* **1984**, *106*, 4632–3. (c) Murch, B. P.; Bradley, F. C.; Boyle, P. D.; Papaefthymiou, V.; Que, L., Jr. *J. Am. Chem. Soc.* **1987**, *109*, 7993–8003.

(14) Loehr, T. M.; Shiemke, A. K. In *Biological Applications of Raman Spectroscopy*; Spiro, T. G., Ed.; Wiley: New York, 1988; Vol. 3, pp 439–90.

(15) (a) Sjöberg, B.-M.; Loehr, T. M.; Sanders-Loehr, J. *Biochemistry* **1982**, *21*, 96–102. (b) Backes, G.; Sahlin, M.; Sjöberg, B.-M.; Loehr, T. M.; Sanders-Loehr, J. *Biochemistry* **1989**, *28*, 1923–9.

(16) (a) Plowman, J. E.; Loehr, T. M.; Schauer, C. K.; Anderson, O. P. *Inorg. Chem.* **1984**, *23*, 3553–9. (b) Solbrig, R. M.; Duff, L. L.; Shriver, D. F.; Klotz, I. M. *J. Inorg. Biochem.* **1982**, *17*, 69–74.

(17) Sanders-Loehr, J.; Wheeler, W. D.; Shiemke, A. K.; Averill, B. A.; Loehr, T. M. *J. Am. Chem. Soc.*, submitted.

(18) Gómez-Romero, P.; DeFotis, G. C.; Jameson, G. B. *J. Am. Chem. Soc.* **1986**, *108*, 851–3.

(19) (a) A computer-assisted literature search (Chemical Abstracts' CAS ONLINE) revealed 52 reported Fe μ-oxo dimers, all of them symmetrical. (b) The following paper describes an unsymmetrical complex: Collamati, I.; Dessy, G.; Fares, V. *Inorg. Chim. Acta* **1986**, *111*, 149–155.

(vs), 1460 (vs), 1390 (m), 1330 (m), 1275 (s), 1090 (m), 1050 (s), 1005 (m), 918 (m), 849 (vs), 832 (vs), 765 (sh), 747 (s), 432 (w), 365 (m).

[N5FeOFeCl$_3$]NO$_3$. To 0.176 g (0.65 mmol) of $FeCl_3 \cdot 6H_2O$ and 0.255 g (0.63 mmol) of $Fe(NO_3)_3 \cdot 9H_2O$ dissolved in 6 mL of 95% ethanol was added 0.313 g of ligand N5 to yield 0.418 g of dark red crystals (75% yield) with an IR spectrum identical with that of the Cl^- analogue except for the NO_3^- band at 1375 cm^{-1}; the nitrate salt is more soluble in acetonitrile than the chloride. Anal. Calcd for $[N5FeOFeCl_3]NO_3 \cdot C_2H_5OH \cdot 2H_2O$, $C_{30}H_{40}N_9O_8Cl_3Fe_2$: C, 41.29; H, 4.62; N, 14.43; Cl 12.18; Fe, 12.80. Found (E+R): C, 41.55; H, 4.23; N, 15.25; Cl, 11.86; Fe, 12.74.

[N5FeOFeBr$_3$]Br. Anhydrous $FeBr_3$ (0.190 g, ca. 0.6 mmol) (Alfa, Lot 101884) was dissolved in 1 mL of ethanol, filtered to eliminate metallic iron impurities, and added to a solution of 0.126 g (0.25 mmol) of ligand N5 in 2 mL of 95% ethanol. After 24 h 0.165 g (64% with respect to N5) of dark red crystals with solubility properties similar to those of the chloro analogue was collected. Anal. Calcd for $[N5FeOFeBr_3]Br \cdot 1.5C_2H_5OH$, $C_{31}H_{39}N_8O_{3.5}Br_4Fe_2$: C, 36.68; H, 3.88; N, 11.08; Br, 31.61; Fe, 11.04. Found (Galbraith): C, 36.41; H, 3.68; N, 11.09; Br, 30.39; Fe, 10.76. Infrared (KBr, cm^{-1}): 3530 (sh), 3350 (s), 3050 (s), 2970 (s), 2920 (s, br), 2780 (sh), 2640 (sh), 1620 (m), 1595 (m), 1545 (m), 1495 (s), 1475 (vs), 1455 (vs), 1390 (m), 1330 (m), 1275 (s), 1090 (m), 1045 (s), 1002 (m), 918 (m), 848 (vs), 831 (vs), 765 (sh), 747 (s), 434 (w), 285 (m).

Isotopic Exchange Experiments. Samples of $[N5Fe^{18}OFeX_3]X$ were prepared from anhydrous FeX_3, X = Cl or Br, in the presence of $H_2{}^{18}O$. Thus, 49 mg (0.30 mmol) of anhydrous $FeCl_3$ was dissolved in 2 mL of absolute ethanol (distilled from magnesium ethoxide) and 0.038 mL of $H_2{}^{18}O$ (97.2 atom %, MSD Isotopes) was added, followed by 128 mg of dried ligand N5 (0.15 mmol). The product contained ca. 80% ^{18}O. Parallel preparations were carried out with regular $H_2{}^{16}O$.

Crystal Structure Analyses. All compounds underwent preliminary studies by means of precession photography with Zr-filtered Mo Kα radiation. Data collection and processing followed the usual procedures.[20] Crystals, sealed in capillaries, were stable to irradiation. Structure solution and refinement used the Structure Determination Package of Enraf-Nonius, as installed on a DEC PDP11/44 computer. Table I contains crystal, data collection, and refinement parameters. All structures were solved with MULTAN82. Hydrogen atoms were included as a fixed contribution to F_{calcd} at their calculated positions and were not refined.

[N5FeOFeCl$_3$]Cl. About half of the H atoms were located from a difference Fourier synthesis. The final difference Fourier map was featureless (largest peak of 0.569 e/Å^3 near the Cl^- counterion). At one solvate site there is well-defined ethanol; at the other a disordered ethanol was fit to the electron density, although microanalysis suggests the likelihood of water at this site. A stereoview of the unit cell contents is shown in Figure S1 (supplementary material). Atomic coordinates and isotropic displacement parameters of non-hydrogen atoms (Table SI), anisotropic displacement parameters (Table SII), and hydrogen atom parameters (Table SIII) are also available as supplementary material.

[N5FeOFeBr$_3$]Br. In the range $30° < 2\theta < 40°$ two forms ($\pm h,+k,+l$ and $\pm h,-k,-l$) were collected and subsequently averaged [$R_{av}(F) = 0.043$ for observed reflections, and 0.081 for all reflections]. The final difference Fourier map was featureless (largest peak of 0.7 e/Å^3 near the Br^- counterion). The crystal structure is isomorphous with the chloro analogue (Figure S2, supplementary material). Atomic coordinates and isotropic displacement parameters of non-hydrogen atoms (Table SIV), anisotropic displacement parameters (Table SV), and hydrogen atom parameters (Table SVI) are also available.

Magnetic Susceptibility. Magnetic susceptibility data were recorded in the range 7–300 K on a SQUID susceptometer Model 905 manufactured by Biomagnetic Technologies Inc. (formerly S.H.E. Corp.). The solid samples were packed into a small aluminum–silicon alloy sample holder (0.75 × 0.45 cm). Data were corrected for the contribution of the quartz bucket holder and for intrinsic diamagnetism by using Pascal's constants, including constitutive corrections.[21] The values used were -5.26×10^{-4} cgsu for the $[N5FeOFeCl_3]Cl$ (as the bis-ethanol salt) and -5.66×10^{-4} cgsu for the bromo analogue. The corrected data were fit to the following general expression incorporated in program MAGNET:[22]

$$\chi(\text{emu mole dimer}^{-1}) = (1 - (x/100))D + (2x/100)M + \text{TIP} \quad (1)$$

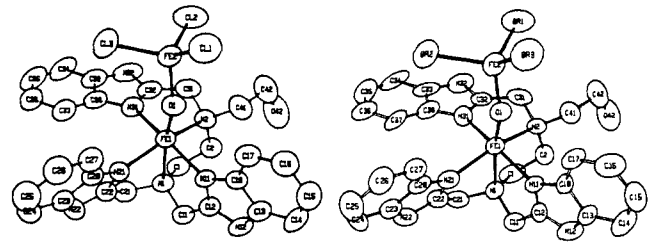

a b

Figure 1. ORTEP perspective diagrams of $[N5FeOFeCl_3]^+$ (a) and of $[N5FeOFeBr_3]^+$ (b). To show the remarkable similarity between the two molecular structures, the pair is presented as a pseudostereodiagram.

D refers to the susceptibility of an exchange-coupled $^5/_2$–$^5/_2$ system (spin Hamiltonian $H = -2JS_1S_2$):[23]

$$D = \frac{0.3753g^2}{T} \frac{2z + 10z^3 + 28z^6 + 60z^{10} + 110z^{15}}{1 + 3z + 5z^3 + 7z^6 + 9z^{10} + 11z^{15}} \quad (\text{where } z = e^{2J/kT}) \quad (2)$$

M represents the Curie–Weiss expression for an $S = {}^5/_2$ impurity with percent mole fraction $2x$, where

$$M = \frac{g^2S(S+1)}{7.9976(T-\theta)} \quad (3)$$

TIP denotes temperature-independent paramagnetism, which for an Fe(III) ion with a ^6A ground term and $g = 2.0$ assumed its expected value of zero. The general approach was to refine x and θ by using low-temperature data (<30 K) and then with these values fixed refine J with higher temperature data. Refinements of all three parameters were also performed, yielding insignificantly different values.

A sample of $[N5FeOFeCl_3]Cl$ was measured initially on a vibrating sample magnetometer between 1.66 and 298 K (see supplementary material, Table SVI and Figure S3).[18] Constitutive corrections were omitted and the value of J was -124 cm^{-1}. When fully corrected and fit to eq 1 the same data yielded a value for J of -120.6 (6) cm^{-1}.

Electronic and Vibrational Spectroscopy. Ultraviolet and visible spectra were recorded on a Hewlett-Packard 8451A diode array spectrophotometer with 1- and 0.2-cm quartz cuvettes. Infrared spectra of KBr pellets were recorded in the range 4000–250 cm^{-1} with a Perkin-Elmer Model 457 spectrophotometer calibrated with standard polystyrene film. The ^{16}O–^{18}O difference spectrum was recorded on a Nicolet 7199 FT-IR. A Jarrell-Ash 25-300 instrument with a Spectra-Physics 164-05 (Ar) laser[16a] was used for Raman spectroscopy. For isotope comparisons, samples were sealed in capillaries and cooled to 90 K by insertion into the cold finger of a glass Dewar filled with liquid nitrogen. To measure the scattering intensity, solid samples were mixed with a known amount of sodium sulfate and run in a spinning sample holder at room temperature with 457.9-nm excitation and a 150° backscattering geometry. Frequencies are corrected with an indene standard.[24]

Mössbauer Spectroscopy. Zero-field spectra were recorded on a conventional constant-acceleration spectrometer with a ^{57}Co γ-ray source. Isomer shifts are relative to metallic iron at room temperature. Other details are described elsewhere.[25] The signal-to-noise ratio at room temperature of the bromo species is poor because of the nonresonant absorption typical for bromine.

Cyclic Voltammetry. Cyclic voltammograms were recorded with a CV27 voltammograph manufactured by Bioanalytical Systems. A three-electrode system was used, consisting of a glassy carbon working electrode, silver–silver chloride reference electrode, and platinum wire as a counter electrode. Potentials are given with respect to the silver–silver chloride electrode.

Results and Discussion

Description of Structures. $[N5FeOFeX_3]^+$: Implications for Methemerythrin. The complexes $[N5FeOFeX_3]X$ (X = Cl, Br) feature unsymmetrical diiron(III) μ-oxo species (Figure 1). One

(20) (a) Gómez-Romero, P.; Jameson, G. B.; Casan-Pastor, N.; Coronado, E.; Beltran, D. *Inorg. Chem.* **1986**, *25*, 3171–6. (b) Hardware setup and software described by: Gabe, E. J.; Le Page, Y.; Grant, D. F. A 4-Circle Diffractometer Control System Written in FORTRAN IV. Chemistry Division, National Research Council of Canada, Ottawa, Canada. April 1980.

(21) Boudreaux, E. A.; Mulay, L. N. *Theory and Applications of Molecular Paramagnetism*; John Wiley & Sons: New York, 1976.

(22) Nonlinear least-squares fitting analysis for corrected molar susceptibilities based on a FORTRAN IV computer program originally written by Marvin Bishop (Columbia University) and generously provided to us by Dr. Kenneth Karlin.

(23) O'Connor, C. J. *Prog. Inorg. Chem.* **1982**, *29*, 203–83.

(24) Hendra, P. J.; Loader, E. J. *Chem. Ind.* **1968**, 718.

(25) Cheng, C.; Reiff, W. M. *Inorg. Chem.* **1977**, *16*, 2097–103.

Table II. Selected Bond Distances (Å) for $[N5FeOFeX_3]^+$

	(a) X = Cl		(b) X = Br
Fe1–O1	1.784 (4)		1.797 (9)
Fe2–O1	1.751 (4)		1.726 (9)
Fe1···Fe2	3.411 (1)		3.408 (3)
Fe1–N1	2.357 (5)		2.34 (1)
Fe1–N2	2.283 (4)		2.28 (1)
Fe1–N11	2.088 (5)		2.084 (8)
Fe1–N21	2.082 (4)		2.09 (1)
Fe1–N31	2.114 (6)		2.107 (8)
Fe2–Cl1	2.201 (3)	–Br3	2.353 (3)
Fe2–Cl2	2.208 (2)	–Br1	2.362 (3)
Fe2–Cl3	2.201 (2)	–Br2	2.329 (3)

Table III. Selected Bond Angles (Degrees) for $[N5FeOFeX_3]^+$

	(a) X = Cl		(b) X = Br
Fe1–O1–Fe2	149.5 (3)	Fe1–O1–Fe2	150.6 (4)
O1–Fe1–N1	172.6 (2)	O1–Fe1–N1	172.7 (3)
O1–Fe1–N2	100.6 (2)	O1–Fe1–N2	100.6 (4)
O1–Fe1–N11	95.9 (2)	O1–Fe1–N11	96.2 (3)
O1–Fe1–N21	108.9 (2)	O1–Fe1–N21	108.6 (4)
O1–Fe1–N31	99.5 (2)	O1–Fe1–N31	99.1 (4)
N1–Fe1–N2	78.0 (2)	N1–Fe1–N2	78.2 (4)
N1–Fe1–N11	76.8 (2)	N1–Fe1–N11	76.6 (3)
N1–Fe1–N21	73.6 (2)	N1–Fe1–N21	73.7 (4)
N1–Fe1–N31	87.5 (2)	N1–Fe1–N31	87.8 (3)
N2–Fe1–N11	89.9 (2)	N2–Fe1–N11	88.9 (4)
N2–Fe1–N21	149.5 (2)	N2–Fe1–N21	150.1 (4)
N2–Fe1–N31	78.3 (2)	N2–Fe1–N31	79.1 (4)
N11–Fe1–N21	94.3 (2)	N11–Fe1–N21	94.3 (4)
N11–Fe1–N31	162.0 (2)	N11–Fe1–N31	162.1 (4)
N21–Fe1—N31	89.4 (2)	N21–Fe1–N31	89.7 (4)
Cl1–Fe2–O1	108.0 (2)	Br3–Fe2–O1	108.7 (2)
Cl2–Fe2–O1	111.2 (2)	Br1–Fe2–O1	112.3 (3)
Cl3–Fe2–O1	107.2 (1)	Br2–Fe2–O1	106.2 (3)
Cl1–Fe2–Cl2	111.81 (9)	Br1–Fe2–Br3	111.2 (1)
Cl1–Fe2–Cl3	111.0 (1)	Br2–Fe2–Br3	110.5 (1)
Cl2–Fe2–Cl3	107.6 (1)	Br1–Fe2–Br2	107.8 (1)

iron atom is hexacoordinate, with the pentadentate ligand N5 and the oxo bridge forming a distorted octahedron; the other iron atom is coordinated to three halo ions and the oxo bridge in a tetrahedral fashion with C_{3v} local symmetry. Overall, the cation molecule possesses no elements of symmetry higher than the identity operator. The chloro and bromo complexes are closely isostructural; indeed the N5Fe moiety maintains its stereochemistry in mononuclear species, such as $[N5FeOC_2H_5]^{2+}$ and $[N5FeCl]^{2+}$.[26]

Selected bond distances and angles are given in Tables II and III, respectively. A comprehensive compilation is available in supplementary material as Tables SVIII and SIX. The tetrahedral Fe–O bonds are slightly shorter than the octahedral Fe–O bonds; the disparity is 0.036 (6) Å for the chloro and 0.071 (13) Å for the bromo species. Both bond lengths, as well as the Fe–O–Fe angle, fall in the range of values observed for symmetrical analogues (Table IV).[1,7] The three Fe–N_{1m} bonds are noticeably shorter than the Fe–N bonds in FeOFe complexes with pyridyl or phenanthroline-derived ligands,[7a,16a,27] and those in an isosceles (μ_3-oxo) triiron(III) cluster featuring an *N*-methylimidazole ligand.[28] The Fe–N_{1m} distances are, however, similar to those observed in several macrocyclic complexes.[29] The equatorial Fe–N_{amine} bonds are similar to those for $[(HEDTA)Fe]_2O^{2+}$,[30] while the Fe–N_{amine} bonds trans to the oxo bridge are unprecedently long. The bond lengths for Fe2–Cl [average 2.213 (7) Å]

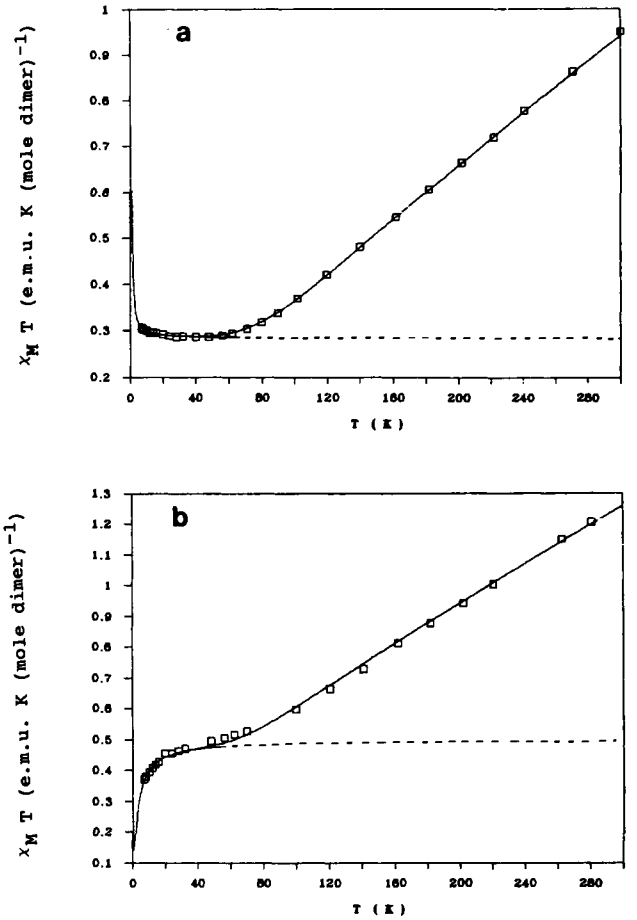

Figure 2. Fit of the corrected magnetic susceptibility data as a function of temperature for $[N5FeOFeX_3]X$. The solid line is the calculated spectrum (see text); the dashed line is the contribution from the paramagnetic impurity. (a) X = Cl; (b) X = Br.

and Fe2–O are identical with those observed in the bis-tetrahedral complex $[Cl_3FeOFeCl_3]$.[2,7b] The Fe–Br_3 fragment has not been characterized previously to our knowledge.

A test for internal consistency on the three imidazole groups showed the scatter of bond distances and angles to be similar to the estimated standard deviations of individual bonds. Crystal packing involves several hydrogen bonds and π–π interactions among benzimidazole moieties, as illustrated in Figures S1 and S2.

The structures of the active centers of methemerythrin and azidomethemerythrin are now known in considerable detail.[31] The average values found for the two forms of the proteins are given in Table IV, together with those of a variety of diiron(III) μ-oxo species. The substantial difference [Δ = 0.24 (6) Å] in Fe–O(oxo) separations seen in two metHr derivatives[31a] is not seen in the more unsymmetrical $[N5FeOFeX_3]^+$ species (Δ = 0.04–0.07 Å) nor in metazido*myo*hemerythrin (Δ = 0.04 Å).[31c] The vibrational spectra of azidomethemerythrin and methemerythrin (see below) are also incompatible with such a large difference in Fe–O bond

(26) (a) Structure and properties of $[N5FeOC_2H_5](ClO_4)_2 \cdot H_2O$: Gómez-Romero, P. Ph.D. Thesis, Georgetown University, 1987. (b) Structure and properties of $[N5FeCl](ClO_4)_2H_3OCl \cdot 2H_2O$: unpublished results.

(27) Healy, P. C.; Skelton, B. W.; White, A. H. *Aust. J. Chem.* **1983**, *36*, 2057–64.

(28) Gorun, S. M.; Lippard, S. J. *J. Am. Chem. Soc.* **1985**, *107*, 4568–70.

(29) (a) Gozens, S.; Peters, R.; Owston, P. G.; Anderson, O. P. *J. Chem. Soc., Chem. Commun.* **1980**, 1199–201. (b) Hoffman, A. B.; Collins, D. M.; Day, V. W.; Fleischer, E. B.; Srivastava, T. S.; Hoard, J. L. *J. Am. Chem. Soc.* **1972**, *94*, 3620–6.

(30) Lippard, S. J.; Schugar, H. J.; Walling, C. *Inorg. Chem.* **1967**, *6*, 1825–31.

(31) (a) Stenkamp, R. E.; Sieker, L. C.; Jensen, L. H. *J. Am. Chem. Soc.* **1984**, *106*, 618–22. (b) Stenkamp, R. E.; Sieker, L. C.; Jensen, L. H.; McCallum, J. D.; Sanders-Loehr, J. *Proc. Natl. Acad. Sci. U.S.A.* **1985**, *82*, 713–6. (c) Sheriff, S.; Hendrickson, W. A.; Smith, J. L. *J. Mol. Biol.* **1987**, *197*, 273–96.

(32) (a) Moss, T. H.; Lillienthal, H. P.; Moleski, C.; Smythe, G. A.; McDaniel, M. C.; Caughey, W. S. *J. Chem. Soc., Chem. Commun.* **1972**, 263–4. (b) Strauss, S. H.; Pawlik, M. J.; Skowyra, J.; Kennedy, J. R.; Anderson, O.; Spartalian, K.; Dye, J. L. *Inorg. Chem.* **1987**, *26*, 724–30. (c) Landrum, J. T.; Grimmett, D.; Haller, K. J.; Scheidt, W. R.; Reed, C. A. *J. Am. Chem. Soc.* **1981**, *103*, 2640–50.

(33) Schugar, H. J.; Rossman, G. R.; Barraclough, C. G.; Gray, H. B. *J. Am. Chem. Soc.* **1972**, *94*, 2683–90.

(34) Petersson, L.; Gräslund, A.; Sjöberg, B.-M.; Reichard, P. *J. Biol. Chem.* **1980**, *255*, 6706–12.

Table IV. Selected Metrical Details and Magnetic Properties of Some μ-Oxo Diiron(III) Species

complex	coord no.	Fe–O, Å	Fe–O–Fe, deg	J, cm^{-1}	I_{as}/I_s[a]	ref
			Singly Bridged Symmetrical			
$[(PP1XDME)Fe]_2O$	5			−131		32a
$[(TPP)Fe]_2O$	5	1.763	174.5	−129		32b
$[(TPC)Fe]_2O$	5	1.747	180	−132		32b
$[(FFPor)Fe]_2O$[b]	5	1.787		−107.5		32c
$[Cl_3Fe]_2O^{2-}$	4	1.755	155.6	−92	0.25	7b
$[(phen)_2(H_2O)Fe]_2O^{4+}$	6	1.785	155.1	−110	<0.04	16a
$[(HEDTA)Fe]_2O^{2-}$	6	1.79	165.0	−95	<0.04	30a, 33
$[LFe(H_2O)_2]_2O$[c]	6	1.773	180	−107	0.16	7a
$[BFe(H_2O)_2]_2O^{4+}$[d]	7	1.8	180	−100		29a
$[(bbimae)FeCl]_2O^{2+}$	6	1.782	180	−103		7c
$[Fe(salen)]_2O$	5	1.78	144.6	−92		35d
$[Fe(3\text{-}t\text{Busaltmen})]_2O$	5	1.779	173.4	−100		35d
			Unsymmetrical			
$[N5FeOFeCl_3]^+$	4	1.751	149.8	−122	4.2	this work
	6	1.782				
$[N5FeOFeBr_3]^+$	4	1.726	150.6	−106	2.4	this work
	6	1.797				
			Triply Bridged			
$[(BPz_3)(OAc)Fe]_2O$	6	1.784	123.6	−121	<0.04	8a
$[(tacn)(OAc)Fe]_2O^2$	6	1.78	118.3	−115[e]	<0.04	9b,c
$\{[(tbpn)(OAc)Fe]_2O\}_2^{2+}$	6	1.794	121.3	−120	0.09	10
$[N3Fe(OAc)]_2O^{2+}$	6	1.785	118.6	−118	<0.04	11
$[N3Fe(OBz)]_2O^{2+}$	6	1.79	118.7	−117	0.08	11
			Diiron Proteins			
metHr	6	1.92	126.5	−134	0.11	31a, 12
	5	1.68				
oxyHr	6			−77	0.17	31b, 12
	6					
azidometHr	6	1.89	134.5		0.27	31a
	6	1.64				
azidometmyoHr	6	1.81	130			31c
	6	1.77				
PAP (bovine spleen)	6?			<−150		4b
	6?					
ribonucleotide reductase				−108	0.20	34

[a] Raman scattering intensity (peak area) of ν_{as}(Fe–O–Fe) relative to ν_s(Fe–O–Fe). Data for unsymmetrical complexes calculated by assuming ν_s at ~425 cm^{-1} (this work). Data for $[Cl_3Fe]_2O^{2-}$ from ref 16b. All other data from ref 17. [b] FFPor denotes a face-to-face, chemically bridged porphyrin. [c] L = 4-chloro-2,6-pyridinedicarboxylate. [d] B is a pentadentate macrocyclic ligand. [e] Reference 9c for the *N,N′,N″*-trimethyl-tacn complex. A value of −84 (1) cm^{-1} has also been reported for parent tacn complex as the iodide salt.[9b]

lengths and make it unlikely that the reported discrepancy is due solely to the asymmetry of the surrounding protein residues. One must question, as did the crystallographers,[31a] whether the observed asymmetry in Fe–O bond distances is in fact real.

Magnetic Susceptibility. For the $[N5FeOFeCl_3]Cl$ the SQUID susceptibility data were fit with $J = -122.3$ (2) cm^{-1}, $x = 3.241$ (5)%, and $\theta = 0.53$ (1) K as shown in Figure 2a. Figure 2b shows the susceptibility vs temperature for the bromo analogue. Considerable difficulty was encountered in preparing acceptably pure samples of the latter. However, similar antiferromagnetic behavior was observed in all samples, with the antiferromagnetic coupling of the bromo species [$J = -106.4$ (9) cm^{-1}, $x = 5.69\%$, $\theta = -2.49$ K] being significantly less than that of the chloro species.

With few exceptions, the coupling constants J for singly bridged μ-oxo diiron(III) species are remarkably independent of the Fe–O–Fe bond angle,[35d] the nature of the ligand, and the coordination number of the iron atoms (4–7).[1,32,35] Values for J in symmetrical Fe–O–Fe systems range from −108 to −131 cm^{-1} for singly bridged iron(III)–porphyrinato species, from −92 to −110 cm^{-1} for singly bridged non-porphyrinato iron complexes, and from −115 to −121 cm^{-1} for triply bridged complexes (Table IV). The stronger coupling exhibited by some of the μ-oxo Fe(III) porphyrinato species has been attributed, in part, to tighter Fe–O binding rather than to the linearity of the Fe–O–Fe unit.[7a] In the non-porphyrinato category, the triply bridged complexes exhibit greater antiferromagnetic coupling (by −5 to −20 cm^{-1}) than that for singly bridged complexes, presumably due to the weak contribution of the two additional carboxylato bridging ligands.[36]

Comparison of the asymmetric complexes with other singly bridged non-porphyrinato iron complexes indicates that the value for J of −122 cm^{-1} for $[N5FeOFeCl_3]Cl$ is anomalously large, whereas that for the stereochemically analogous bromo complex is more normal. A value of −127 (1) cm^{-1} has been observed for the asymmetric complex $[N6FeOFeCl_3]Cl\cdot{}^1/_2HCl\cdot 3H_2O\cdot 2C_2H_5OH$ [N6 = *N,N,N′,N′*-(tetrabenzimidazolylmethyl)diaminoethane] which is similar in structure and spectroscopic properties to the N5 analogue, but only three of the four benzimidazole groups coordinate.[37] The unusually large J values observed for these asymmetric complexes could be a function either of bond lengths (Table IV) or, more likely, of the asymmetry itself. It is of interest that purple acid phosphatase, which has an even

(35) (a) Helms, J. H.; ter Haar, L. W.; Hatfield, W. E.; Harris, D. L.; Jayaraj, K.; Toney, G. E.; Gold, A.; Mewborn, T. D.; Pemberton, J. R. *Inorg. Chem.* **1986**, *25*, 2334–7. (b) Ercolani, C.; Gardini, M.; Murray, K. S.; Pennesi, G.; Rossi, G. *Inorg. Chem.* **1986**, *25*, 3972–6. (c) Kennedy, B. J.; Murray, K. S.; Zwack, P. R.; Homborg, H.; Kalz, W. *Inorg. Chem.* **1985**, *24*, 3302–5. (d) Mukherjee, R. N.; Stack, T. D. P.; Holm, R. H. *J. Am. Chem. Soc.* **1988**, *110*, 1850–61.

(36) (a) Lippard, S. J. *Angew. Chem., Int. Ed. Engl.* **1988**, *27*, 344–52. (b) Thich, J. A.; Toby, B. H.; Powers, D. A.; Potenza, J. A.; Schugar, H. J. *Inorg. Chem.* **1981**, *20*, 3314–7. (c) Reem, R. C.; Solomon, E. I. *J. Am. Chem. Soc.* **1987**, *109*, 1216–26.

(37) Gõmez-Romero, P.; Witten, E. H.; Reiff, W. M.; Jameson, G. B. To be submitted for publication in *Inorg. Chem.*

(38) (a) Kadish, K. M.; Larson, G.; Lexa, D.; Momenteau, M. *J. Am. Chem. Soc.* **1975**, *97*, 282–8. (b) Wenk, S. E.; Schultz, F. A. *J. Electroanal. Chem.* **1979**, *101*, 89–99.

(39) Shiemke, A. K.; Loehr, T. M.; Sanders-Loehr, J. *J. Am. Chem. Soc.* **1986**, *108*, 2437–43.

(40) Maroney, M. J.; Kurtz, D. M., Jr.; Nocek, J. M.; Pearce, L. L.; Que, L., Jr. *J. Am. Chem. Soc.* **1986**, *108*, 6871–9.

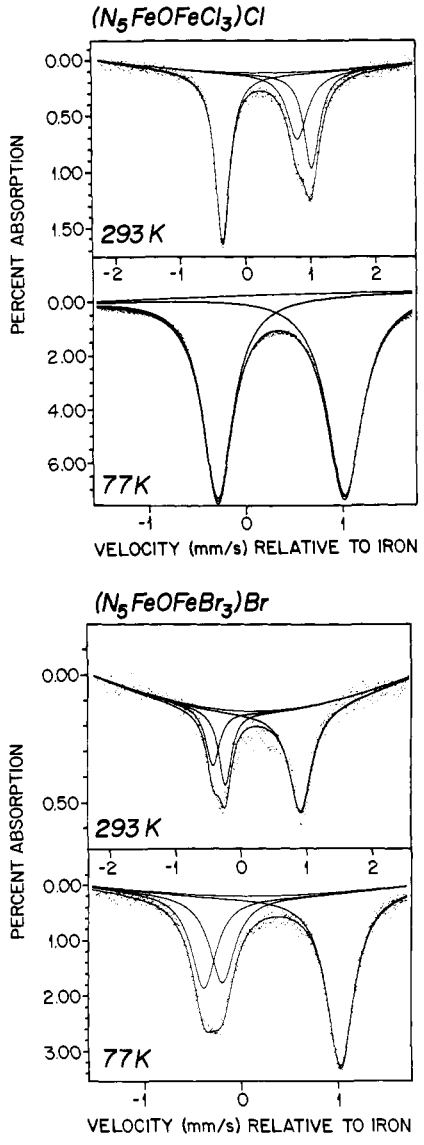

Figure 3. Mössbauer spectrum of $[N5FeOFeX_3]X$ at 293 and 77 K. (a) (top) X = Cl; (b) (bottom) X = Br. Note that for (a) at 77 K the quadrupole doublets are perfectly overlapped.

larger value of $-J > 150$ cm^{-1}, is also known to have an asymmetric dinuclear iron site.[4]

Mössbauer Spectra. The asymmetric nature of the dinuclear species $[N5FeOFeCl_3]Cl$ is apparent in the room-temperature ^{57}Fe Mössbauer spectra, where two quadrupole doublets of essentially equal area are partially overlapped. However, at 77 K the doublets are completely overlapped—absence of evidence for asymmetry cannot be taken as evidence of absence, at least for a single temperature measurement. The bromo complex has a different temperature dependence such that there is less overlap of doublets at 77 K compared to the chloro analogue. See Figure 3.

The spectra for the chloro and bromo diiron species could not be reliably deconvoluted with four Lorentzian functions because of the near-perfect overlap of absorptions. Thus, the following isomer shifts and quadrupole splittings are derived from fits with three Lorentzian functions for which the χ-squared values are ~500. For the chloro complex at 293 K, $\delta = 0.23$ and $\Delta E_q = 1.15$ mm/s ($FeOCl_3$), and $\delta = 0.34$ and ΔE_q 1.36 mm/s (FeON5). For the bromo complex at 77 K, $\delta = 0.31$ and $\Delta E_q = 1.41$ mm/s ($FeOBr_3$), and $\delta = 0.41$ and $\Delta E_q = 1.22$ mm/s (FeON5). The smaller of the two isomer shifts and its associated quadrupole splitting are typical of tetrahedral iron.[7b,41] For the octahedral iron, the isomer shift lies at the low end of the range observed in symmetrical bis-octahedral diiron(III) μ-oxo species.[41] In oxyhemerythrin and in some but not all forms of methemerythrin, the native B2 component of ribonucleotide reductase, and purple acid phosphatase, a pair of quadrupole doublets are seen with isomer shifts in the range 0.45–0.55 mm/s and quadrupole splittings spread over a remarkably wide range of 1.0–2.5 mm/s.[2] The fact that the coupled irons in the proteins show a greater difference in quadrupole splitting (range in ΔE_q of 0.33–0.87 mm/s) than is observed for the coupled iron atoms in the asymmetric $[N5FeOFeX_3]X$ complexes (range in ΔE_q of 0.19–0.21 mm/s) proves that there is a significant amount of asymmetry in the ligand environments of all these dinuclear iron proteins.

Table V. Summary of Electronic Spectra for N5 Complexes in Acetonitrile

compound	λ, nm	ϵ^a
$[N5FeOFeCl_3]NO_3$	327	5700
	360 (sh)	3600
	400 (sh)	2100
	540 (sh)	210
	655 (sh)	60
$[N5FeOFeBr_3]Br$	350	4300
	420 (sh)	2600
	550 (sh)	200
$[N5FeOC_2H_5](ClO_4)_2$[b]	384	410
	550 (sh)	50
	650	45
	750	45
$[N5FeCl](ClO_4)_2$[b]	328	4200
	470	3050

[a] L(mol of Fe)$^{-1}$ cm^{-1}. [b] Reference 26.

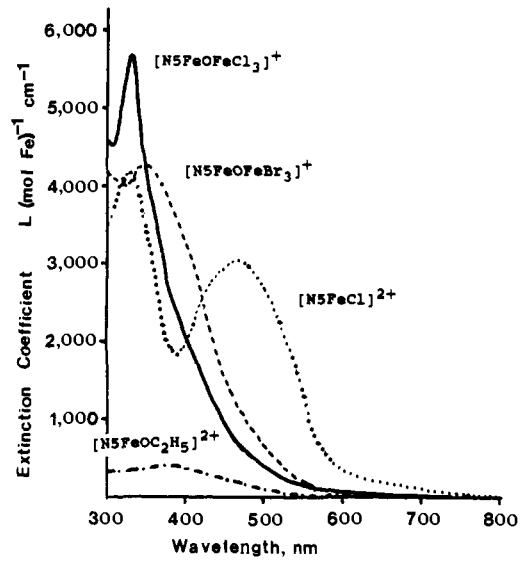

Figure 4. UV-visible spectra for $[N5FeOFeX_3]^+$, X = Cl (a), Br (b), $[N5FeOC_2H_5]^{2+}$ (c), and $[N5FeCl]^{2+}$ (d).

Electronic Spectra. Assignment of Significant Features. Electronic spectral data for complexes are summarized in Figure 4 and Table V. The dominant feature at 327 nm for $[N5FeOFeCl_3]^+$ is assigned to a predominantly $Cl^- \rightarrow$ Fe(III) charge-transfer (CT) transition, by comparison with the mononuclear complex $[N5FeCl]^{2+}$,[26] which has a band at 328 nm, and also with $(Cl_3Fe)_2O^{2-}$ and $FeCl_4^-$.[7b,42] For the bromo complex the band at 350 nm involves, at least in part, a $Br^- \rightarrow$ Fe(III) CT transition, consistent with the lower ionization potential of Br^- compared to Cl^-.[43]

On the basis of Raman excitation profiles for the Fe–O–Fe vibration,[17] the oxo → Fe(III) CT band has been identified at 360–420 nm in the spectra of hemerythrin, ribonucleotide re-

(41) Gibb, T. C.; Greenwood, N. N. In *Mössbauer Spectroscopy*; Chapman and Hall: London, 1971.

(42) Neuse, E. W.; Meirim, M. G. *Transition Met. Chem.* **1984**, *9*, 205–8.

(43) Cotton, F. A. *Advanced Inorganic Chemistry*, 4th ed.; J. Wiley & Sons: New York, 1980.

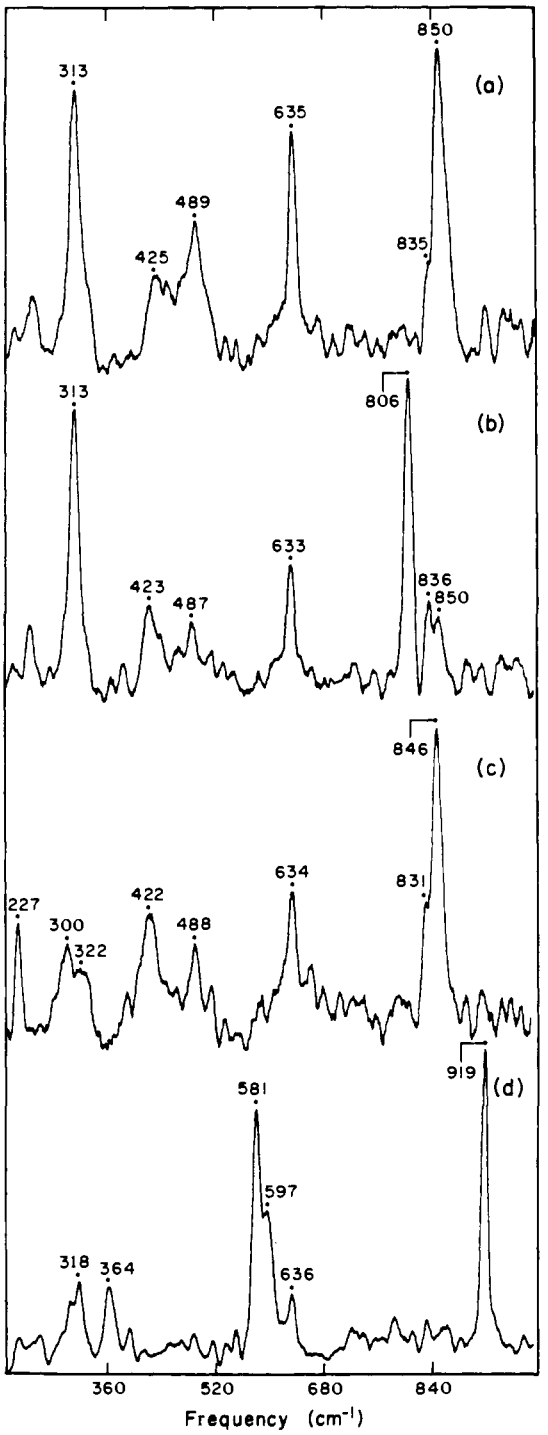

Figure 5. Resonance Raman spectra of $[N5Fe^{16}OFeCl_3]Cl$ (a), $[N5Fe^{18}OFeCl_3]Cl$ (b), $[N5FeOFeBr_3]Br$ (c), and $[N5FeOC_2H_5][ClO_4]_2$ (d). Samples were sealed in capillaries at 90 K and illuminated in a 150° backscattering geometry with 488.0-nm (50-mW) excitation, 6-cm^{-1} slit, and 1 cm^{-1} s^{-1} scan rate for a total of six scans.

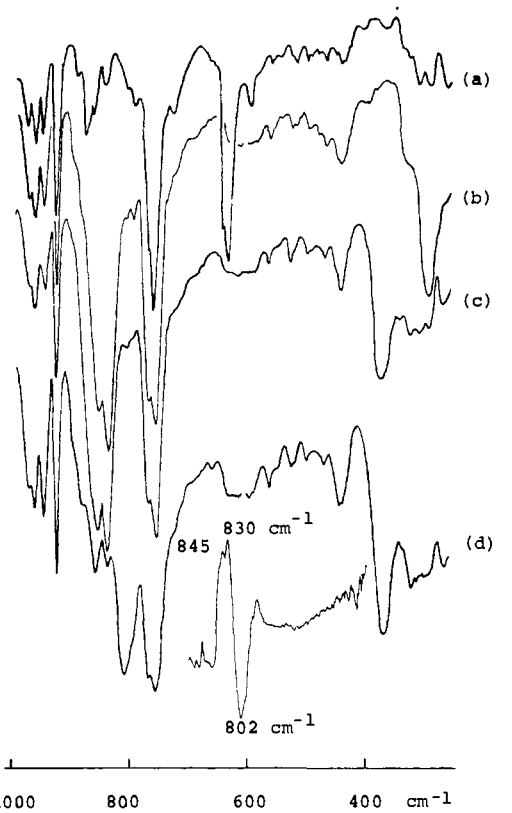

Figure 6. Infrared spectra (KBr pellets) of $[N5FeOC_2H_5][ClO_4]_2$ (a), and of $[N5FeOFeX_3]X$, X = Br (b), X = Cl (c), in the region 1000–250 cm^{-1}. The spectrum of the ^{18}O-exchanged chloro complex is shown in (d). The inset shows the difference spectrum (d) − (c) obtained with an FT-IR spectrometer in the region 400–950 cm^{-1}.

ductase, and a number of dinuclear iron model complexes. The shoulder at ~360 nm for $[N5FeOFeCl_3]^+$ may be associated with this transition. Its weakness is consistent with the poor resonance enhancement of Fe–O–Fe vibrational modes (see below). In the case of the bromo complex, this band is lost under the $Br^- \rightarrow$ Fe(III) CT band. The band at ~400 nm, common to diiron and monoiron complexes of N5, is assigned to a LMCT involving primarily the nitrogen donor atoms of N5.

IR and Resonance Raman Spectra. Assignment of Fe–O and Fe–X Modes. In the absence of coupling to other modes, nonlinear Fe–O–Fe moieties with Fe–O–Fe bond angles of ~150° should exhibit only three nondegenerate vibrational modes: ν_{as}(Fe–O–Fe) at ~840 cm^{-1}, ν_s(Fe–O–Fe) at ~450 cm^{-1}, and δ(Fe–O–Fe) at ~100 cm^{-1}.[17,44] The dominant feature in the resonance Raman spectra of $[N5Fe^{16}OFeX_3]^+$ is a single band at 850 cm^{-1} (X = Cl) (Figure 5). This band, which shifts by −44 cm^{-1} upon substitution of ^{16}O by ^{18}O, is assigned to ν_{as}(Fe–O–Fe). No distinct mode is clearly assignable to a symmetric Fe–O–Fe stretch in either the IR or resonance Raman spectrum—the latter is in contradistinction to almost all other (symmetrical) μ-oxo diiron(III) complexes for which the Raman-active band, ν_s(Fe–O–Fe), in the range 360–545 cm^{-1} is strongly resonance-enhanced and the ν_{as}(Fe–O–Fe) mode is very weak.[8a,16,17] In $[N5FeOFeCl_3]Cl$ the features at 425, 499, and 635 cm^{-1} all appear to shift by −2 cm^{-1} upon substitution with ^{18}O. On the basis of the known Fe–O–Fe angle of 150°, the feature at 425 cm^{-1} is likely to have the most ν_s(Fe–O–Fe) character. The enhancement of the 425-cm^{-1} manifold is low, with the molar scattering intensity only ~5-fold greater than that of the ν_1 mode of sulfate. Most Fe–O–Fe model compounds exhibit symmetric stretches with 10- to 100-fold greater molar scattering than sulfate, while for hemerythrin and ribonucleotide reductase this value ranges from 300 to 1000.[17]

The unusually strong enhancement of the ν_{as}(Fe–O–Fe) mode for unsymmetrical complexes is documented in Table IV. For symmetrical, monobridged complexes a maximal ν_{as}/ν_s intensity ratio of 0.25 is observed, whereas in the unsymmetrical, monobridged complexes the intensity ratios are 10- to 20-fold higher. For the symmetrical triply bridged complexes this ratio appears to be consistently less than 0.10. A doubly bridged complex $[(TPA)_2Fe_2O(OBz)]^{3+}$, has been described recently in which the two TPA (tripyridineamine) ligands are unsymmetrically coordinated with respect to the dinuclear iron cluster.[45] This com-

(44) Czernuszewicz, R. S.; Sheats, J. E.; Spiro, T. G. *Inorg. Chem.* **1987**, *26*, 2063–7.

(45) Yan, S.; Norman, R. E.; Que, L., Jr.; Backes, G.; Ling, J.; Sanders-Loehr, J.; Zhang, J. M.; O'Connor, C. J., manuscript submitted.

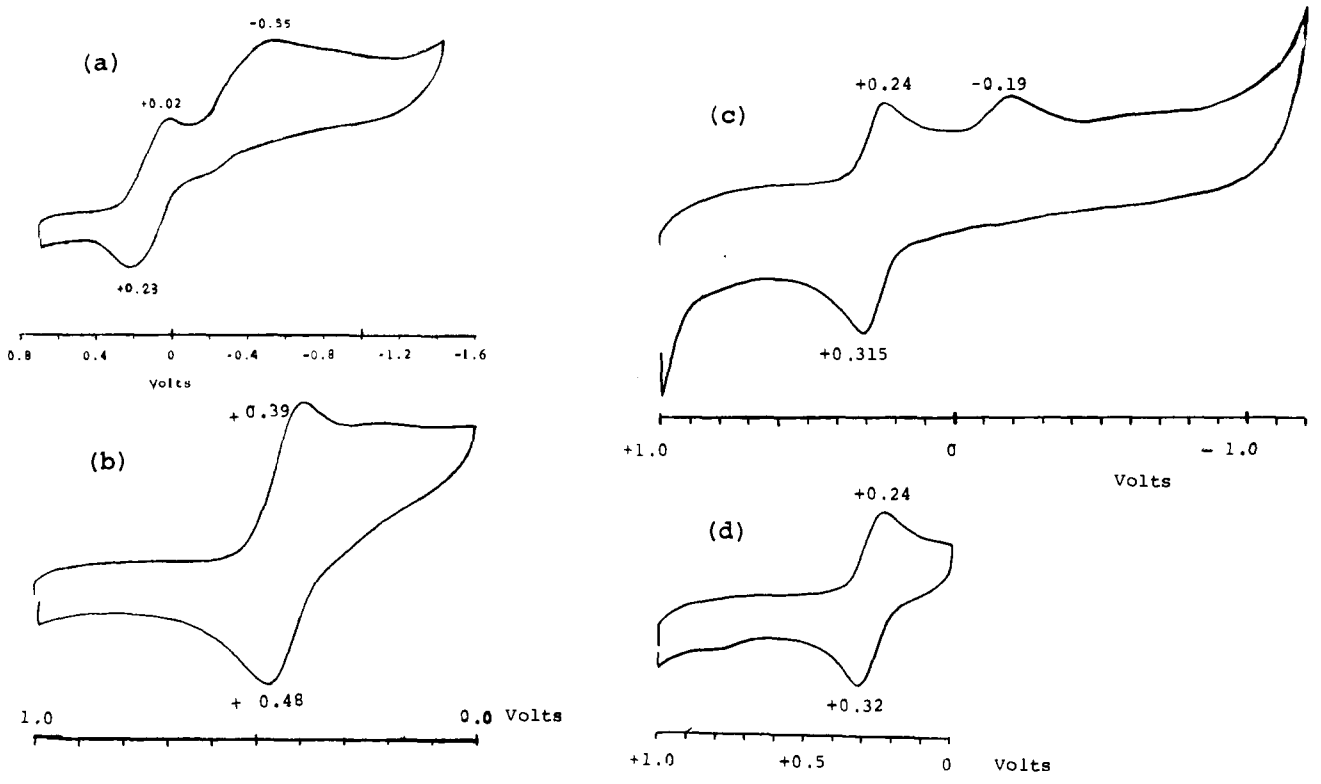

Figure 7. Cyclic voltammograms of (a) $[N5FeOFeCl_3]^+$ 9.8×10^{-04} M (CH_3CN solution and $LiClO_4$ supporting electrolyte), (b) $[N5FeOC_2H_5]^{2+}$ 3.3×10^{-04} M (CH_3CN solution and $(TBA)ClO_4$ supporting electrolyte), (c) $[N5FeOFeBr_3]^+$ 3.5×10^{-04} M aqueous solution (1 M HOAc/NaOAc, pH 5.03) and (d) $[N5FeOC_2H_5]^{2+}$ 1.7×10^{-04} M aqueous solution (2 M HOAc/NaOAc, pH 5.04).

pound has two distinct Fe–μ-O distances of 1.77 and 1.81 Å and a ν_{as}/ν_s intensity ratio of 0.33 that is 3-fold higher than that of symmetrical multiply bridged species. Since the inequality of the Fe–μ-O distances in the TPA complex is similar to that in the unsymmetrical monobridged complexes, the *unprecedented observation for* $[N5FeOFeX_3]^+$ *complexes that* ν_{as}*(Fe–O–Fe) is 2- to 4-fold more intense than* ν_s*(Fe–O–Fe) is likely to be related to the greater asymmetry of the Fe–O–Fe′ moiety.*

In hemerythrin the exogenous ligand binds to only one of the two triply bridged iron atoms.[31] The relatively high intensities for ν_{as} in several forms of metHr compared to the triply bridged models (Table IV) are consistent with this variability in ligand environment. Moreover, the reported 0.25-Å differences in Fe–μ-O distances for various metHr derivatives[31a] seem inconsistent with the low overall enhancement of ν_{as} relative to ν_s. Finally the ν_{as}/ν_s intensity ratio of ribonucleotide reductase is consistent with the asymmetry at the dinuclear iron site inferred from Mössbauer spectroscopic studies.[46]

For bovine spleen purple acid phosphatase, magnetic susceptibility data indicate the presence of a μ-oxo moiety, whereas in the resonance Raman spectrum, the ν_s(Fe–O–Fe) mode, usually strongly enhanced in oxo-bridged dinuclear iron proteins, is not apparent. The absence of an imidazole trans to the oxo bridge has been proposed as one reason for weak enhancement of this mode.[4b,17] Another reason could be the known asymmetric distribution of tyrosine ligands in purple acid phosphatase.[4] Although the asymmetric complexes show a greater intensity for ν_{as}(Fe–O–Fe) than for ν_s(Fe–O–Fe), the enhancements of both of these modes are so weak that they would be difficult to detect at the concentrations available for protein samples.

Infrared bands at 365 cm^{-1} ($[N5FeOFeCl_3]^+$) and 285 cm^{-1} ($[N5FeOFeBr_3]^+$) are assigned to the respective Fe–X_3 asymmetric stretch by comparison with $(Cl_3Fe)_2O^{2-}$.[7b] Resonance Raman bands at 313 cm^{-1} ($[N5FeOFeCl_3]^+$) and 226 cm^{-1} ($[N5FeOFeBr_3]^+$) are assigned similarly[16b] to the symmetric Fe–X_3 mode. In the region where ν_{as}(Fe–O–Fe) is expected in the infrared spectrum, a very strong doublet is seen at about 830 and 850 cm^{-1} for $[N5Fe^{16}OFeX_3]^+$ (Figure 6). Upon exchange with ^{18}O both peaks decrease in intensity, while a broad band grows at 802 cm^{-1}. The 830-cm^{-1} component that is intense only in the IR spectrum is attributed to a coupled Fe–O–Fe and FeN5 vibration.[47] Its low intensity in the Raman spectrum is the result of the weak resonance enhancement of FeN5 modes compared to Fe–O–Fe or FeX_3 modes. This trend is apparent when the IR and Raman spectra of these dinuclear species are compared with the spectra (Figures 5d and 6a) of the mononuclear species $[N5FeOC_2H_5][ClO_4]_2$, for which the stereochemistry of the N5FeO moiety is very similar to that observed for the dinuclear complexes.[26] Whereas, for example, the band at 916 cm^{-1} is present in the infrared spectra of mono- and dinuclear species, this band is readily identifiable in the resonance Raman spectrum of only the mononuclear species. This is consistent with the oxo → Fe(III) and X^- → Fe(III) CT transitions dominating the absorption spectrum in the visible region.

Cyclic Voltammetry and Stability of Dinuclear Species in Solution. Parts a and b of Figure 7 show cyclic voltammograms of N5 complexes in acetonitrile and water, respectively. In acetonitrile solutions of the complex $[N5FeOFeCl_3]^+$, one-electron waves for a quasi-reversible ($E_{1/2}$ = 0.125 V) and an irreversible reduction are observed. The redox pair in the same solvent for the related mononuclear complex $[N5FeOC_2H_5]^{2+}$ is reversible and appears at $E_{1/2}$ = 0.435 V. Thus, the N5Fe moiety in the dinuclear complex is the one reduced and the integrity of the complex is maintained. In water the first reduction wave of the dimeric species $[N5FeOFeBr_3]^+$ is identical with the one from the monomer in the same solvent and buffer, indicating that dissociation of the complex takes place under those conditions.

(46) Atkin, C. L.; Thelander, L.; Reichard, P.; Lang, G. *J. Biol. Chem.* **1973**, *248*, 7464–72.

(47) This is not unprecedented: see, for example: (a) Fleischer, E. B.; Srivastava, T. S. *J. Am. Chem. Soc.* **1969**, *91*, 2403–5. (b) Cohen, I. A. *J. Am. Chem.* Soc. **1969**, *91*, 1980–3. (c) Burke, J. M.; Kincaid, J. R.; Spiro, T. G. *J. Am. Chem. Soc.* **1978**, *100*, 6077–83. (d) Takenaka, A.; Takeuchi, S.; Kobayashi, Y.; Itoh, K. *Surf. Sci.* **1985**, *158*, 359–69.

From the small paramagnetic shifts seen in ^1H NMR spectra,[48] the intensity and insensitivity of the extinction coefficient of the 325-nm band to dilution, and the presence of the very strong doublet (850 and 834 cm^{-1}) also observed in the infrared spectrum of $[N5FeOFeCl_3]^+$ dissolved as the NO_3^- salt in acetonitrile solution, we infer that the unsymmetrical species $[N5FeOFeX_3]^+$ (X = Cl, Br) maintain their integrity in acetonitrile solution. In solvents with better donor capabilities, such as DMSO and water, they disintegrate yielding mononuclear species. The presence of the quasi-reversible reduction wave in the CV of the chloro complex in acetonitrile implies the existence of a stable Fe(II)-Fe(III) mixed-valence species. These results with $[N5FeOFeCl_3]^+$ represent the first demonstration of a mixed-valence complex in a singly bridged μ-oxo diiron(III) system with a neutral chelate—mixed-valence species have been reported for the *N,N'*-ethylenebis(salicylideniminato) complex $[Fe(salen)]_2O$ and tetraphenylporphyrinato complex $[Fe(TPP)]_2O$.[38] Mixed-valence species are well-known for trinuclear iron complexes with μ_3-oxo and bis(μ-carboxylato) bridges,[49] and stable Fe(II)···Fe(III) complexes have been isolated by use of a binucleating ligand with a bridging phenoxide group.[50] A transient mixed-valence species has also been observed for the triply bridged $[Fe_2O(OAc)_2(tacn)_2]^{2+}$ complex by cyclic voltammetry.[51] This oxidation level is considerably more prevalent in the μ-oxo-bridged proteins. Mixed-valence intermediates are readily observed in hemerythrin and methane monooxygenase by EPR spectroscopy.[2,3a,6] For purple acid phosphatase, the Fe(II)···Fe(III) state is actually the active form of the enzyme.[4]

Conclusions

The first nonbiological, unsymmetrical μ-oxo diiron(III) complexes have been characterized. As such, they provide unique information relevant to the understanding of the physical and chemical properties of dinuclear iron proteins whose active centers consist of two nonequivalent iron atoms. First, we find that the $Fe-O_{oxo}$ bond lengths are only slightly perturbed by asymmetry, while at appropriate temperatures the asymmetry is clearly apparent in the Mössbauer spectra. Second, the asymmetry leads to a strongly active ν_{as}(Fe–O–Fe) mode in both the infrared and Raman spectrum. Third, the intensity of the oxo → Fe(III) CT band and the related resonance enhancement of the ν_s(Fe–O–Fe) mode appear to be diminished. Finally, the antiferromagnetic coupling for $[N5FeOFeCl_3]Cl$ is anomalously large by comparison with salts of symmetrical complexes, $[Cl_3FeOFeCl_3]^{2-}$, and, for example, $[(phen)_2(H_2O)Fe(phen)_2(H_2O)]$, that possess ligands identical with or closely analogous to those around the iron centers of the unsymmetrical dinuclear species.

The dinuclear iron proteins hemerythrin (Hr), ribonucleotide reductase (RR), and purple acid phosphatase (PAP) exhibit many of these same features, which are significantly different from the properties of symmetrical oxo-bridged model complexes. These include markedly different Mössbauer quadrupole splitting for the two iron atoms in Hr, RR, and PAP, enhanced Raman intensities for ν_{as}(Fe–O–Fe) in Hr and RR, lack of electronic or Raman evidence for an oxo bridge in PAP, and unusually large antiferromagnetic coupling constants for Hr and PAP. In addition, the ability of $[N5FeOFeCl_3]^+$ to form a one-electron-reduced species in acetonitrile is reminiscent of the behavior of Hr, PAP, and methane monooxygenase.[2] These results suggest that the asymmetry, which is clearly present at the dinuclear iron sites of Hr, RR, and PAP, may be important in determining the types of redox chemistry these sites undergo.

Acknowledgment. We thank the National Institutes of Health for support through Grants 5R01 DK37702-02 (G.B.J.) and GM 18865 (J.S.-L), the National Science Foundation Solid State Chemistry Program Grant DMR 8313710 (W.M.R.), and the Comite Conjunto Hispano-Norteamericano para la Cooperacion Cultural y Educativa for a fellowship awarded to P.G.-R. We thank Mr. John Donovan for the careful synthesis of a highly ^{18}O-substituted sample of $[N5FeOFeCl_3]Cl$, Professor Ekk Sinn and Dr. T. Thanyasiri for the measurement of magnetic susceptibility data on the SQUID susceptometer, Dr. William D. Wheeler for Raman measurements, and Dr. Nieves Casañ-Pastor for recording the NMR spectra and cyclic voltammograms.

Supplementary Material Available: Tables of non-hydrogen atomic coordinates and isotropic displacement parameters, anisotropic atomic displacement factors, and hydrogen atom parameters for $[N5FeOFeCl_3]Cl$ (Tables SI–SIII, respectively) and $[N5FeOFeBr_3]Br$ (Tables SIV–SVI, respectively), magnetic susceptibility data (Table SVII), complete listing of bond distances (Table SVIII), and complete listing of bond angles (Table SIX) for $[N5FeOFeBr_3]Br$, unit cell stereodiagrams for $[N5FeOFeCl_3]Cl$ and $[N5FeOFeBr_3]Br$ (Figures S1 and S2, respectively), fit of magnetic susceptibility data (vibrating sample susceptometer) for $[N5FeOFeCl_3]Cl\cdot 2C_2H_5OH$ (Figure S3), and UV–visible spectra (19 pages). Ordering information is given on any current masthead page.

(48) Gómez-Romero, P.; Morris, N. L.; Ben-Hussein, A.; Jameson, G. B., manuscript in preparation.

(49) Woehler, S. E.; Wittebort, R. J.; Oh, S. M.; Kambara, T.; Hendrickson, D. N.; Inriss, D.; Strouse, C. E. *J. Am. Chem. Soc.* **1987**, *109*, 1063–72.

(50) (a) Suzuki, M.; Uehara, A.; Endo, K. *Inorg. Chim. Acta* **1986**, *123*, L9–11. (b) Borovik, A. S.; Que, L., Jr. *J. Am. Chem. Soc.* **1988**, *110*, 2345–7. (c) Ben-Hussein, A.; Morris, N. L.; Gómez-Romero, P.; Jameson, G. B. *Inorg. Chem.*, submitted.

(51) Hartman, J. R.; Rardin, R. L.; Chaudhuri, P.; Pohl, K.; Wieghardt, K.; Nuber, B.; Weiss, J.; Papaefthymiou, G. C.; Frankel, R. B.; Lippard, S. J. *J. Am. Chem. Soc.* **1987**, *109*, 7387–96.